Magazine of Civil Engineering

ISSN 2712-8172

journal homepage: http://engstroy.spbstu.ru/

DOI: 10.34910/MCE.109.14

Fibers reinforcement of the fissured clayey soil by desiccation

M. Jamei*, ***Y. Elassaf***, ***A. Ahmed***, ***A. Mabrouk***

Northern Border University, Engineering College, Arar, Kingdom Saudi Arabia (KSA)

**E-mail: mehjamei@yahoo.fr*

Keywords: desiccation, cracks, fibers, tensile strength, modeling

Abstract. The cracks caused by desiccation induce rapid failures as rapid shallow landslides in stiff and fragile clayey soils. Several environmental structures such as landfill liners and road embankments are often constructed by compaction of a series of soil layers. These works suffered in many cases of disorders due to desiccation. One of the potential valuable techniques to reduce these disorders is the short fibers reinforcement. Fibers reduce the cracks propagation and the geometric cracks characteristics such as the length, depth and opening. The paper presents an experimental characterization of the crack pattern observed in compacted samples at optimum water content (OMC) with and without fibers reinforcement. 2D Image Analysis has been used to investigate the characteristics of the geometric cracks. Alfa natural short fibers used to assure the reinforcement, reduced the carks' propagation by stopping the propagation and reducing their 3D opening (surface opening and depth growth). The role of fibers to improve the tensile strength and reduce the growth of the crack has been well-highlighted. At this stage, a simple model was calibrated to predict the tensile strength for reinforced soil specimens with short fibers considering various fibers contents and fiber's geometrical characteristics.

1. Introduction

The unsaturated soil mechanics offers a convenient framework for understanding several disorders due to the collapse, swelling, and shrinkage by saturation changes. This paper focuses on the constrained shrinkage role in developing cracks in soils. In order to reduce the developed cracks, micro-reinforcement is often helpful. So, the use of short fibers is one of the recommended techniques. This paper investigates this role and presents experimental evidence to prove fibers' role. It also presents a simple model to predict the tensile strength as a key parameter governing the cracks' appearance and propagation.

Otherwise, several engineering works suffer from the disorders caused by the wetting-drying environmental cycles. The long drying path affected the geotechnical works built in fine soils as embankments, slopes, shallow foundations, and landfill liner cover, which causes cracks development. Cracks reduce mechanical properties such as stiffness, cohesion, and shear resistance. It significantly increases permeability, which permits a high seepage and infiltration of rainwater. Many disorders were previously studied concerning seepage and cracks [1–3]. For example, in the case of landfill liners, [4] affirmed that cracks deteriorate the liner containment function leading to accentuated leachate migration into surrounding soils and groundwater. On the other hand, several researchers were concerned by the behavior of compacted intact unsaturated clay samples and highlighted the role of the fabric on the macroscopic behavior (see, for instance, [5]). For example, it was shown that the tensile resistance depended on the fabric structure, which was conditioned by the compaction path. Depending on the fabric structure, this behavior is responsible for the cracks pattern type and cracks growth. Moreover, the effect of the wetting-drying cycles after compaction is crucial in the crack's development and cracks pattern characteristics evolution [6]. The paper [7] has shown that the crack intensity factor for wet-dry cycles was higher than those obtained for the compaction-dry cycle (samples were dried immediately after compaction

Jamei, M., Elassaf, Y., Ahmed, A., Mabrouk, A. Fibers reinforcement of the fissured clayey soil by desiccation. Magazine of Civil Engineering. 2022. 109(1). Article No. 10914. DOI: 10.34910/MCE.109.14

and then submitted to wetting-dry cycles). Studying the impact of wetting-drying cycles on the crack's development [6] showed that the growth of the cracks significantly affects both the unsaturated permeability of the studied fine soil and the water retention property. Well recently, [8] provided an overview of the desiccation process of fine soils, summarizing the experimental development in the laboratories and the field to investigate and characterize the cracks and the main models proposed to follow the development and propagation of the crack. The authors concluded that, although cracks in soils have been widely studied, there are still some aspects, principally: the establishment of reliable relationships between the cracking parameters and macroscopic engineering parameters; the investigation of the relation between the microstructure of fine soils and cracking parameters and particularly with its dynamic process. The engineering field's expectations of studying the geotechnical's stability investigate the cracked soils under desiccation process considering the effect of wetting-drying cycles.

On the other hand, few studies were interested in using the micro-reinforcement technique to improve the desiccated clays submitted to wetting-drying cycles (see, for instance, [9]). However, the use of short fibers for intact soils to reinforce the shear strength was more studied [10, 11]. In addition, fibers reinforcement concrete was well studied (see non-exhaustive works [12–14])

This paper presents the tensile feature and cracks development during the drying path of a typical fine soil characterized by a high percentage of fines based on experimental tests using a new tensile device with suction control. The data was required during the experience, and many sequential photos were taken at a fixed time interval. These photos have been exploited separately by the image analysis. Added to this first series of tests, samples were prepared by mixing the soil with natural Alfa short fibers. The mixing was conducted in a completely dry state, and the water was added progressively until reaching the optimum water content of the composite. In this paper, the role of the fibers on the cracks growing is investigated. Since the tensile strength is the main resistance material that governs the development of the cracks, this research determined water content variation by using a controlled-displacement direct tensile. A simple analytical model was calibrated to predict the tensile strength. Predicting the growth and propagation of cracks and the fiber's role in reducing and delaying the cracks is a challenge of this study.

2. Materials and Methods

2.1. Soil Properties

The selected soil was classified using Standard ASTM classification (USCS) as silty-clay soil with high plasticity. The physical properties are summarized in Table 1. Moreover, the soil exhibits high shrinkage potential [15]. The tested soils' physical and chemical propertiess are summarized in Table 1.

Table 1. Main physical characteristics of the studied soil.

Bulk Density (gr/cm^3)	LL (%)	PL (%)	PI (%)	SL (%)	VBS
2.65	60	35	25	13	7

The activity of the studied soil is defined by equation (1):

$$A = \frac{PI}{\%\ of\ \ fines \prec 2\mu m} = \frac{25}{32.5} = 0.77 \quad (1)$$

The activity of used soil is classified as normal, and it appears in the range of the Illite clays. However, as is shown in Figure 2, the smectite fraction is more dominant. A standard Proctor test have been performed, which gave the compaction curve. The maximum dry density was 1.52 gr/cm^3, and the optimum water content was 25 % (Figure1).

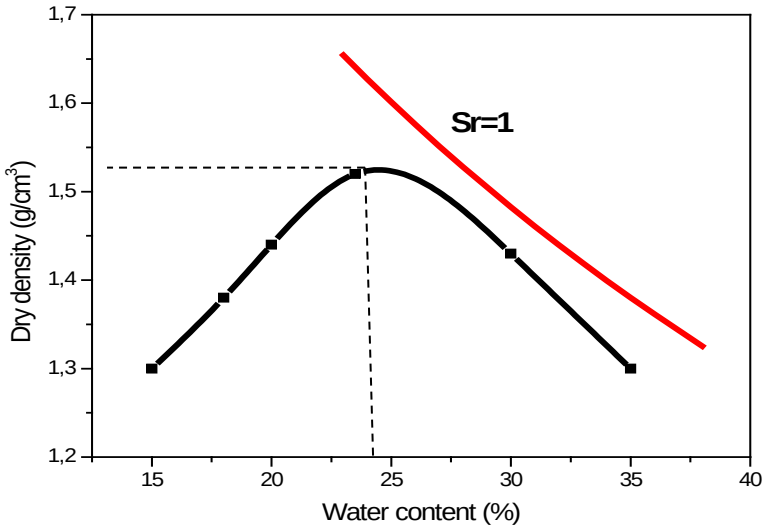

Figure 1. Compaction curve of the used soil (Sr= degree of saturation).

The grain size distribution (GSD) as provided by the laser technique is also summarized in Table 2. Since fine-grained soils are more susceptible to crack due to small pores [7], the compaction at the OMC is more convenient to investigate the crack pattern growth and its consequences on the fundamental hydromechanical properties of shear resistance and permeability. Figure 2 shows the XRD distribution, which indicates the dominant smectite component (see table 2, in which the clay fractions are summarized).

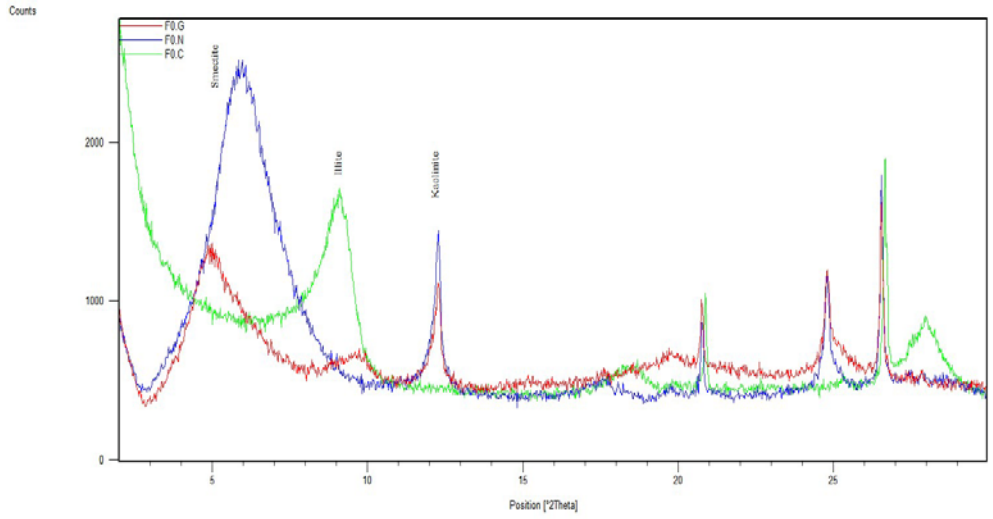

Figure 2. XRD results for the undistributed sample.

Table2. Grain Size and XRD Analysis.

Fraction of soil	Sand (15%)	Silt (50%)	Clay (35%)
Mineral component	Smectite (62 %)	Illite (22 %)	Kaolinite (16%)

In the unsaturated state, the water retention curves linking the water content (or saturation degree) to the suction are fundamental property. So, in this study, the water retention curves have been determined (Figure 3) using different techniques as the osmotic technique, the salt solutions, and the psychrometer [16]. The principal water retention curves were obtained for different paths. The first was obtained from slurry samples submitted to the drying path (D) and the compacted drying path (CD). The compacted samples are prepared at OMC state. A humidification path was applied from OMC to the saturation water content of 30%. A drying path was applied from 30% (CD) water content. According to the experimental results, the van-Genuchten model [17] was used to fit the experimental results (Eq. 2). As shown in Figure 3, the effect of the initial state of the soil has an essential effect on the water retention curve (WRC), where

the WRC of slurry and dried soil is entirely different from WRC compacted and dried. This happened due to the microstructure change by mechanical compaction compared to the evolution of the slurry one, which is influenced by the only hydraulic drying path. It is evident that such hydraulic retention behavior affects both the tensile strength and soil microstructure (see for instance [5]) and consequently the cracks network growth and development.

$$\omega(s) = \left[\omega_r + \frac{(\omega_s - \omega_r)}{\left[1 + (\frac{s}{a})^n\right]^m} \right] \quad (2)$$

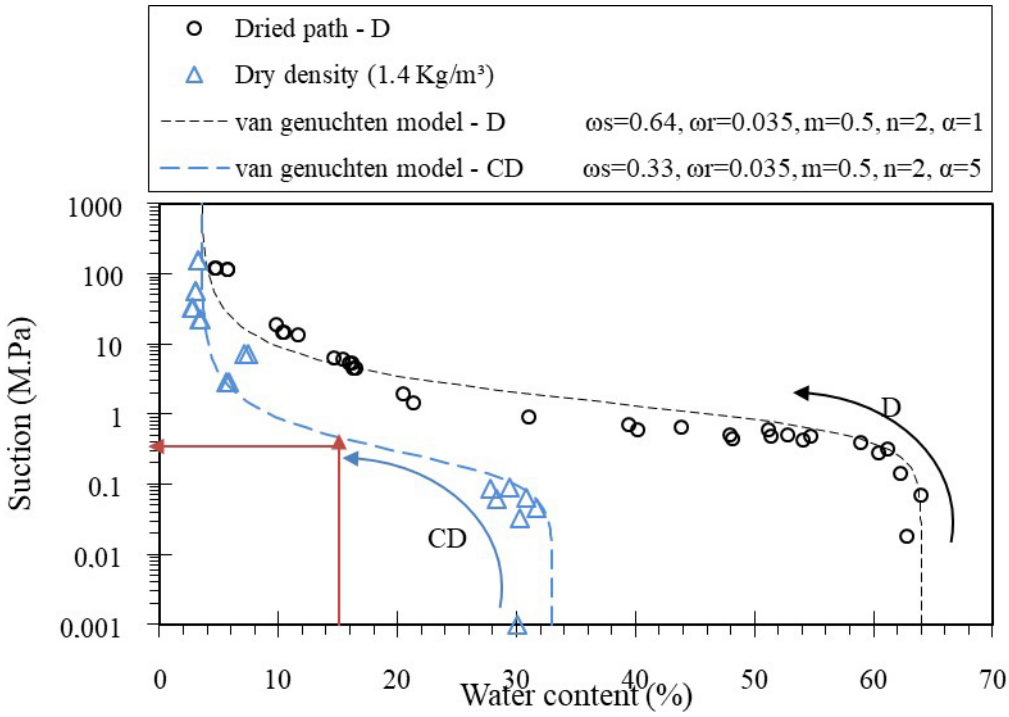

Figure 3. Principle Drying Water retention curves for compacted-drying (CD) and slurry-drying (D) samples.

2.2. Fibers Properties

Alfa fibers were selected as natural fibers to assure the micro-improvement of tensile strength of soil and then delay the rise and the growth of cracks and even affect their orientation and opening. Natural Alfa fibers were selected due to their abundance in Tunisia (especially in the west). In this study, Alfa fibers were treated using Sodium hydroxide. This chemical treatment was used to facilitate the extraction of fibers from the plants' branches and was developed to have a less aggressive extraction. It consists of degrading the non-cellulosic constituents of the plant, taking into account adequacy, rapidity, and preservation of the properties of the fibers, and respecting environmental requirements, of course [9]. This extraction was carried out by Alfa rods soaking in beakers with a soda solution (2N) and at a temperature of 100 °C. After the time determined for soaking (2h), the fibers were removed from the beakers and rinsed several times with distilled water to remove any trace of NaOH solution from the fibers. Figure 4 gives real and MEB photos of Alfa fibers.

Regarding international research [10, 18–20], some studies have been conducted using different natural fibers for tens of years. Among them, sisal fibers have equivalent physical, chemical, and mechanical properties. Table 3 summarizes the properties of Alfa fibers compared to those of Sisal fibers as also vegetal fibers mainly produced in Brazil and in some countries in the South of America.

Table 3. Physical and mechanical properties of Alfa and Sisal fibers.

Properties	Sisal [a]	Alfa[b]
Stiffness E_f (GPa)	11.8	13
Tensile Strength $\sigma_t(MPa)$	510	565
Breaking Deformation ε_f(%)	5.6	5.8
Density (gr/cm^3)	0.94	0.89
Average Diameter (mm)	0.3	0.3
Acid and alkali resistance	Very	good
Dispersibility	Normal	

[a][18], [b][21].

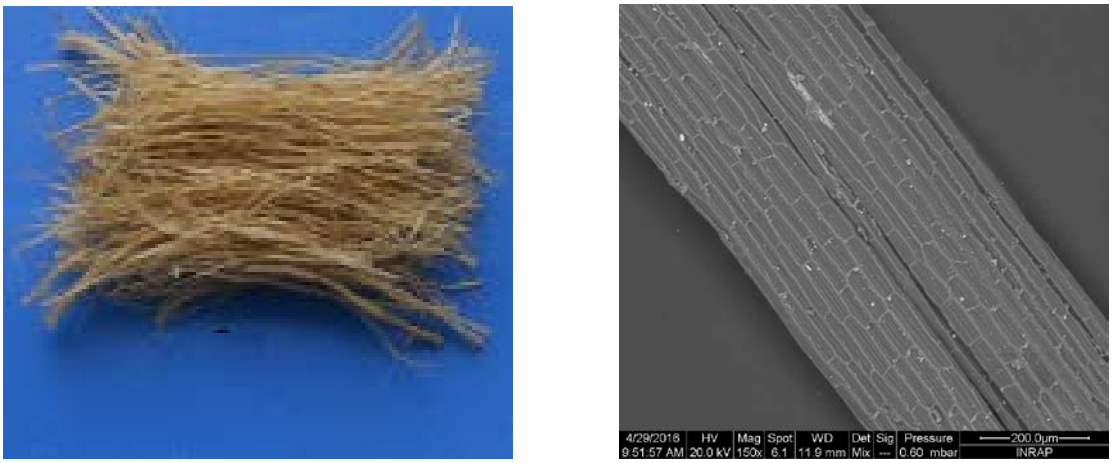

(a) **(b)**

Figure 4. Alfa fibers (a) and the corresponding MEB observation (x150) (b).

Figure 5 gives the microscopic observation of Halfa fibers used as natural fibers to reduce the propagation of desiccation cracks. The microscopic observation shows the adhesion between the soil and the fibers, which contributes to developing more tensile deformation to composite soil during the developed tensile by the constrained shrinkage.

Figure 5. MEB observation (x150) of the Alfa fiber embedded in the used soil: a good adhesion between soil and fibers.

2.3. Tensile Experience

A new direct tensile device was developed based on the transformation of the shear box and using a specific mold to prepare the sample for the tensile action (Figure 6). This required a specific methodology to perform the compaction in the mold. In fact, firstly, the specimens were prepared by hand mixing to assure the homogeneity of dry soil and distilled water content concerning the amount of water to reach the

OMC value in each test. For the second set of reinforced specimens, a fixed volumetric rate (η_f) of fibers to dry soil and distilled water was added for each test. A test campaign was carried out with η_f =0.1%; η_f =0.3% and η_f =0.5%, as defined by Eq. 3.

$$\eta_f = \frac{m_f}{m_{sd}}, \tag{3}$$

where m_f and m_{sd} are respectively the masses of fibers and dry soil used to prepare the specimen.

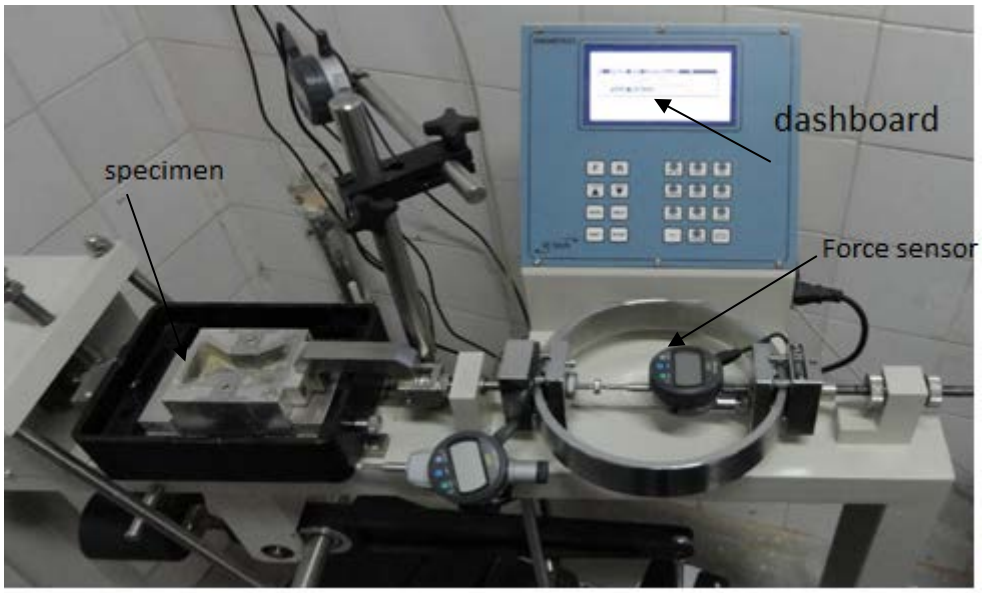

Figure 6. Photo of direct tensile test used in this study

2.4. Desiccation tests

Several authors recently studied desiccation-induced cracks using image analysis [22, 23]. New test setups and methodologies were developed, except that few have studied the 3D cracks growth [24]. According to a fixed time step, the crack patterns were quantitively determined by image analysis basing on the surface photos token progressively during the drying process. Different authors have used several parameters to characterize the crack pattern (see [25, 26]): crack spacing and depth and average crack width opening. This study characterized the cracks pattern principally by the Crack Intensity Factor (CIF). CIF is the area of cracks for the total area. The image analysis involved the conversion of the digital image from the original RGB (red-green-blue) color to gray-scale and then to a binary black and white image obtained by the principle of 'threshold gray-scale image.' After that, the binary image's black and white pixels were quantified. The white pixels correspond to the undamaged zone, while the black pixels correspond to the cracks. Each quantified number of pixels gave the corresponding density CIF [7, 25–27].

3. Results and Discussions

3.1. Tensile strength for nonreinforced soil: Effect of drying path

Figure 7 gives the tensile strength results against the compacted water content (more or less 6 tests were conducted for each path: Standard Proctor compaction and compaction-drying paths). As shown in this figure, the trend of the tensile strength against the water content depends on the followed path, particularly the compaction trend of tensile strength-suction has a similar to the Proctor compaction one [9–28]. The tensile strength of specimens prepared at a fixed initial water content of 80% OMC and dried increases and reaches a constant value of 120 kPa for suction of 60MPa.

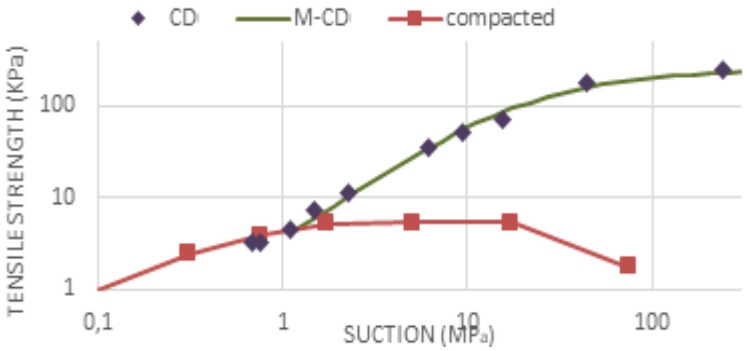

Figure 7. Tensile strength against suction for different paths (C: Compacted; CD: compacted and dried, M-CD modeled or fitted experimental results).

3.2. Experimental results of Tensile strength for reinforced soil

Figure 8 shows the typical tensile curves of specimens with different fibers rates (η_f = 0.1 %; η_f = 0.3 % and η_f = 0.5 %. The length of all used Alfa fibers was 30 mm). The specimens were compacted in the tensile box, where the dry density was fixed at 1.5 gr/cm^3. As expected, the tensile strength (the pick corresponding to the maximum of tensile stress) increases with fiber rate η_f and the delayed cracks initiation. After the reached pick value, the tensile stress decreased suddenly. Probably, the fibers played a weak role after they reached maximum tensile stress. Both phenomena were observed, the fiber's slippage and breaking of the rest.

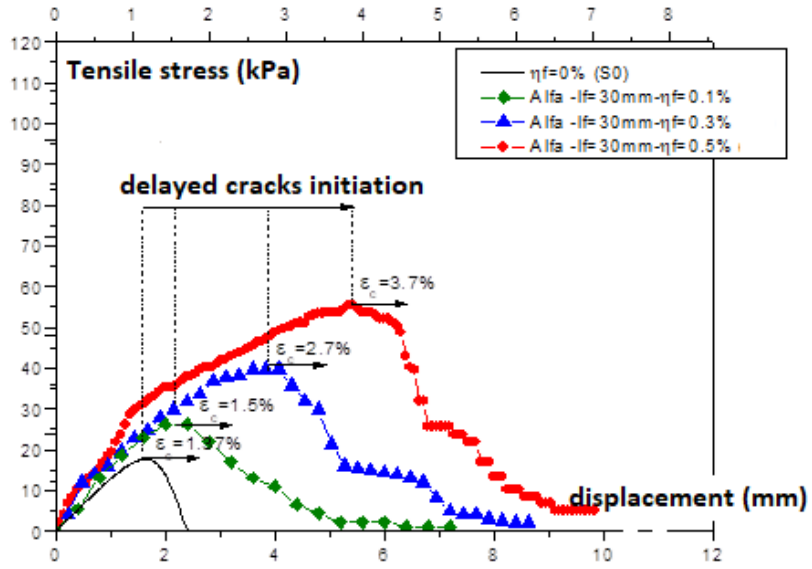

Figure 8. Tensile stress evolution with axial deformation for different fibers contents.

Several authors identified that the crack initiation is linked to the fact that the tensile stress developed by shrinkage (under drying) exceeded or equaled the tensile strength. Locally the failure was developed, and the crack growth is happened due to the tensile energy concentration [29–30]. In addition, when the fibers content increases, cracks initiation is more delayed. Appeared the first crack, with the same opening, by direct tensile force, was observed for 3.7% of tensile deformation with η_f = 0.5 %. However, it appears for 1.5 % of deformation for η_f = 0.1% (Figure 7). Consequently, the contribution of the fibers has been mainly noted for both mechanical properties, the increase of tensile resistance, and the delay of the fissure opening.

3.3. Modeling of the tensile strength of reinforced specimens

Because of the importance of developing modeling to predict the cracks, which first begins with predicting the tensile strength, we propose a simple model that can be considered in this section. As follow

the tensile strength $\sigma_t(s)$ which depends on the suction (s) can be upper-estimated using the Coulomb criterion (Eq.4):

$$\sigma_t(suction,\eta_f)=\sigma_t(s,\eta_f)=\cot an(\varphi(s,\eta_f)).C(s,\eta_f) \quad (4)$$

where $\varphi(s,\eta_f)$ and $C(s,\eta_f)$ are respectively the friction angle and cohesion of the unreinforced soil, depending on both the suction (s) and fibers content (η_f).

Then, using the water retention curve, corresponding to the compacted and dried path (CD), one obtains the suction corresponding to the OMC (25 %), of 0.5MPa (Figure 3). Thus, the value of the measured tensile strength corresponding to the suction of 0.5MPawas deduced from the results in Figure 7. The tensile strength was of 8 kPa. However, from the direct compaction test (where) the compaction was done in the tensile device followed by a tensile test gives a tensile strength of 14 kPa. This difference is attributed to the compaction path with or without drying path. The 14 kPa value corresponds to the compaction at Standard Optimum Proctor without drying, and the experimental strength value was obtained from a direct test on the specimens at OMC (without a drying following the compaction).

Considering that determining the tensile strength using the model by equation (4) needs the triaxial tests under suction control on reinforced specimens. Therefore, we propose a model based on the direct tensile tests where the tensile strength $\sigma_{ts}(s,\eta_f)$ for reinforced specimen is given as follow (Eq. 5):

$$\sigma_{ts}(s,\eta_f)=\sigma_{ts}(s,\eta_f=0)+\Delta\sigma_{ts}(s,\eta_f) \quad (5)$$

where
$$\Delta\sigma_{ts}(s,\eta_f)=\frac{\alpha\pi D_f\sum_{i=1}^{N_f}(\sigma_t(\varepsilon_f(s,\eta_f))(l_a)_i)}{A} \quad (6)$$

and
$$\alpha=\frac{\int_{-\frac{\theta}{2}}^{\frac{\theta}{2}}(d\theta)}{2\pi} \quad (7)$$

where D_f is the diameter of the fiber, $\sigma_t\left(\varepsilon_f(s,\eta_f)\right)$ is the tensile stress at the failure strain $\sigma_t\left(\varepsilon_f(s,\eta_f)\right)$ which obviously depends on the suction and fibers content. A is the section of the interest zone (20mmx30mm, see Figure 9). $(l_a)_i$ is the active length of fiber (i) under tensile. In general, it was assumed that this active length is in the range between L/4 and L/2. It is fixed in this model at L/4 for all the fibers in the zone's interest. Also, because only a part of the set of fibers is submitted to tension, a coefficient (α) defining an effective zone (see Figure 9), where fibers are submitted in tension, is introduced and defined by α (Eq. 7).

The number of fibers N_f is deduced from the volumetric fibers content given as follow (Eq. 8):

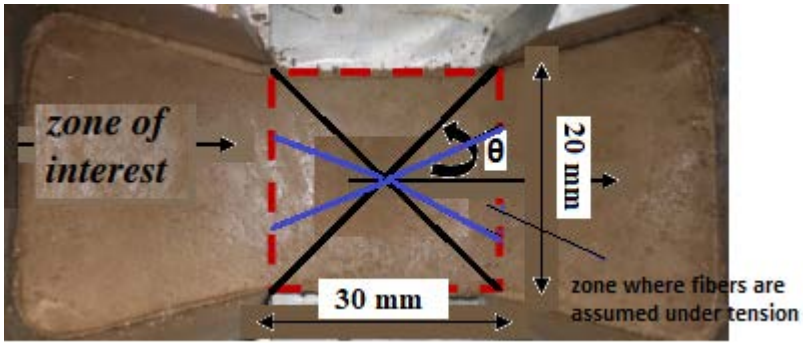

Figure 9. Shema of the interest of the specimen in tensile box.

$$N_f=N_v.V_{zI} \quad (8)$$

where V_{ZI} = volume of zone of interest =20 mm×30 mm×20 mm and N_V is the number of fibers per unit of volume. N_V is given as follow (Eq. 9), as it was shown in [10]:

$$N_v = \frac{C_f}{(1+C_f)L\pi r^2} \text{ where } C_f = \eta_f \frac{\gamma_d}{\gamma_f} \tag{9}$$

With γ_d is the maximum dry density of soil (at OMC) and γ_f is the density of Alfa fibers (see Table 3). The term corresponds to a coefficient indicating the part of a set of fibers assumed to be submitted to tensile. The fibers under tensile are elastically deformed, and the tensile stress developed by each fiber is as follow:

$$\sigma_t(\varepsilon_f(s,\eta_f)) = E_f\ \varepsilon_c(s,\eta_f) \tag{10}$$

where E_f is the stiffness of Alfa fiber (Table 3) and $\varepsilon_c(s,\eta_f)$ is the strain at maximum tensile stress of the reinforced specimen at given suction (s) and fiber content (η_f), (Figure 8).

Figure 9 gives the predicted tensile strength of the composite (reinforced soil) against measured tensile strength. This figure highlights a good agreement between the model and the experience's results (the correlation coefficient was 0.96).

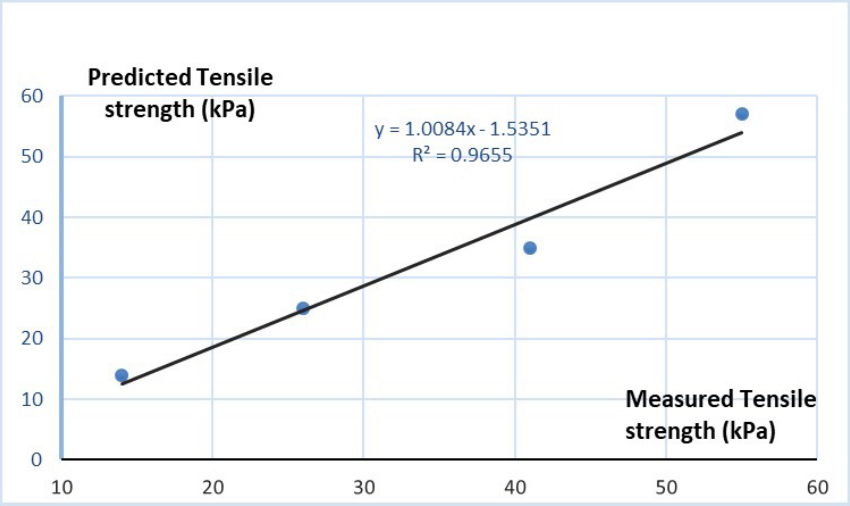

Figure 9. Predicted Tensile strength against the measured tensile strength.

3.4. Role of fibers in Cracks development

The Cracks Influence Factor (CIF) has been defined as the following (Eq. 11). CIF has been considered the main parameter to measure the cracks propagation by measuring the surface opening considered as the area of total cracks captured by the vertical camera that took the images sequentially. Figures 10.a, 10.b and 10.c give respectively the images of cracks patterns in three-time sequences (t = 48 h, t = 60 h and t = 72 h), for non-reinforced and reinforced specimens (η_f = 0.3 % and η_f = 0.5 %).

$$CIF(\%) = \frac{Fissure's\ Area}{Total\ Area\ of\ the\ specimen} \tag{11}$$

As shown in Figure 10.a, the opening of primary cracks reached its final state at 60 hours. However, secondary cracks continue to appear without a significant effect on the value of the area of the total fissure.

t = 48 h t = 60 h t = 72 h

Figure 10. a cracks pattern evolution by drying (nonreinforced specimen).

t = 48 h t = 60 h t = 72 h

Figure 10. b cracks pattern evolution by drying (reinforced specimen η_f = 0.3 %)

t=48h t=60h t=42h

Figure 10.c cracks pattern evolution by drying (reinforced specimen η_f = 0.5 %)

The formation and the morphology were well affected by the fibers. The same conclusion was given by [31]. Without fibers (nonreinforced clay), the cells tend to be more significant. Large opening and orthogonal and non-orthogonal carks have been observed. The orthogonal cracks were well-identified for the nonreinforced specimen. However, the fiber affects either the crack intensity by reducing the opening and the length of cracks and the morphology of patterns, which were developed with discontinues aspect and not necessarily perpendicular.

Figure 11 gives the variation of CIF during drying. Although the effect of fibers in cracks opening is well-demonstrated, where the role of fibers was to stop the opening, their growth was also well affected. The first fissure was happened at 2hours and was well larger for the nonreinforced specimen. However, with significantly smaller dimensions (width and length), the first one was better for the reinforced specimen (η_f = 0.5 %).

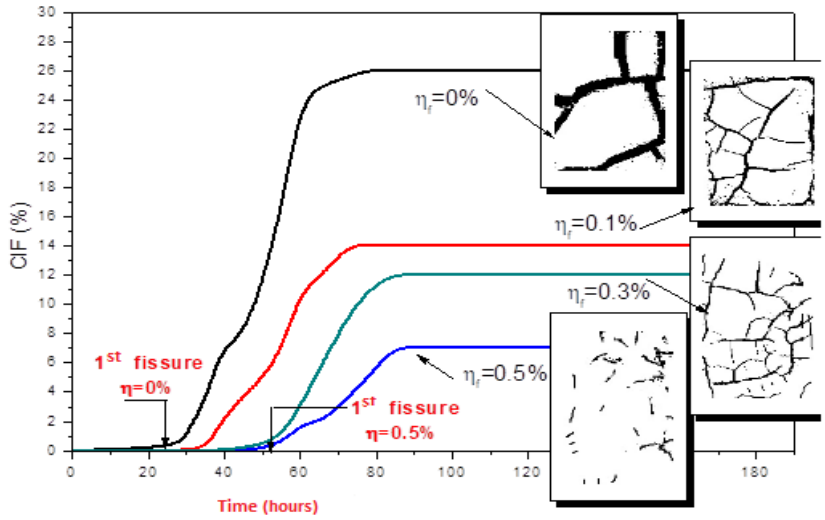

Figure 11. CIF evolution during drying time: Effect of fibers content.

The CIF was reduced from 26 % (non-reinforced clay) to 14 %, 12 % and 6 % for respectively η_f = 0.1 %, η_f = 0.3 % and η_f = 0.5 %. The fibers not only influenced the intensity factor, but also the formation and morphology of the cracks.

From the literature, the governing mechanism of desiccation of unreinforced soils (mainly silty soils) has been analyzed based on the experiments and image analysis [32–36]. As stated, the cracks birth arrived when strained shrinkage develops tensile stress that exceeds the tensile resistance of the material. Now regarding the role of fibers to globally increases the tensile strength and locally to develop a tensile force that opposes the forces developed by strained shrinkage, the fibers reduce the cracks growing and development and modify their orientation.

4. Conclusions

In this paper, the cracking patterns and morphology have been studied in the laboratory using rectangular specimens of plastic clayey-silty soil. The Digital Image Correlation (DIC) was used to quantify the cracks patterns (Length and Opening) parameters. The CIF parameter as a dimensionless parameter was retained in this study to quantify the cracks growing and development during the drying process. This study leads to the following results:

1. The tensile strength and its relation with the suction were obtained for this soil using direct tensile tests. The trends of tensile strength-suction were: (a) the same as the Proctor-compaction curve for the compacted specimens. However, for the compacted and dried specimens (b), the tensile strength against suction had a completely different trend. This indicated a monotonic increase of tensile strength with an increase of suction.

2. From DIC, the morphology of the pattern of the cracks was well-investigated. For nonreinforced specimens, the cells were large, and the opening of cracks was also significant. However, the cells vanished progressively with the increase of fibers content. The morphology of the crack pattern was significantly affected by the fibers. The presence of fibers omitted the perpendicular morphology.

3. Because the fibers improved the tensile strength, the cracks intensity (measured by CIF) was significantly decreased by adding the fibers.

4. From an environmental point of view, the use of natural short fibers seems to be a promising alternative for geotechnical works which suffer from desiccation by drying. In arid regions, such technical solutions will be envisaged and encouraged.

5. Although experimental results have been obtained for many soils by research, mainly in laboratories, the reinforced soils by fibers are still few studied. Some aspects still need more attention: (a) The quantitative relations between the fibers content, the fibers length, the fibers sections, and separately the tensile strength for soils with initial water contents and dry densities. (b) the same relations are still needed with the cracks parameters characteristics. (c) the modeling of each relation helps to obtain an efficiency model to predict the role of fibers by delaying the inevitable cracks and eventually stopping them from growth, which should be paid more attention.

References

1. Willden, R., Mabey, D.R. Giant desiccation fissures on the black rock and smoke creek deserts, Nevada. Science. 1961. Vol. 133. No. 3461. Pp. 1359–1360.
2. Morris, P.H., Graham, J., Williams, D.J. Cracking in drying soils. Canadian Geotechnical Journal. 1992. Vol. 29. No. 2. Pp. 262–277.
3. Tay, Y.Y., Stewart, D.I., Cousens, T.W. Shrinkage and desiccation cracking in bentonite-sand landfill liners. Engineering Geology. 2001. Vol. 60. No. 1–4. Pp. 263–274.
4. Miller, C.J., Mishra, M. Modeling of leakage through cracked clay liners — I: state of the art. Water Resources Bulletin. 1989. AWRA 25 (3). Pp. 551–555.
5. Trabelsi, H., Romero, E., Jamei, M. Tensile strength during drying of remolded and compacted clay: The role of fabric and water retention. Applied Clay Science. 2018. 162. Pp. 57–68.
6. Louati, F., Trabelsi, H., Jamei, M., Taibi, S. Impact of wetting-drying cycles and cracks on the permeability of compacted clayey soil. European Journal of Environmental and Civil Engineering. 2019. 1. Pp. 1–26. DOI: 10.1080/19648189.2018.1541144
7. Yessiller, N., Miller, C.J., Inci, G., Yaldo, K. Desiccation and cracking behavior of three compacted landfill liner soils. Engineering geology. 2000. Vol. 57. No. 1-2. Pp. 105–121.
8. Wei, X., Gao, C., Liu, K. A Review of Cracking Behavior and Mechanism in Clayey Soils Related to Desiccation. Advances in Civil Engineering. 2020. Vol. 2020. Pp. 1–12. Article ID 8880873. DOI: 10.1155/2020/8880873
9. Chebbi, M., Guiras, H., Jamei, M. Tensile behaviour analysis of compacted clayey soil reinforced with natural and synthetic fibers: effect of initial compaction conditions. European Journal of Environmental and Civil Engineering. 2017. 24:3. Pp. 354–380. DOI: 10.1080/19648189.2017.1384762
10. Jamei, M., Villard, P., Guiras, H. Shear Failure Criterion Based on Experimental and Modeling Results for Fiber-Reinforced Clay, International Journal of Geomechanics. 2013. December. Vol. 13. No. 6. Pp. 882–893.
11. Polyankin, A.G., Korolev, K.V.,Kuznetsov, A.O. Analysis of reinforced soil sustainability while tunnel construction. Magazine of Civil Engineering. 2020. 95(3). Pp. 80–89. DOI: 10.18720/MCE.95.8
12. Eberhardt, E., Stead, D., Stimpson, B., R.S. Read Identifying crack initiation and propagation thresholds in brittle rock. Can. Geotech. 1998. J. 35. Pp. 222–233.
13. Begich, Y.E., Klyuev, S.V., Jos, V.A., Cherkashin, A.V. Fine-grained concrete with various types of fibers. Magazine of Civil Engineering. 2020. 97(5). Article No. 9702. DOI: 10.18720/MCE.97.2
14. Gavrilov, T.A., Kolesnikov, G.N., Evolving crack influence on the strength of frozen sand soils. Magazine of Civil Engineering. 2020. 94(2). Pp. 54–64. DOI: 10.18720/MCE.94.5
15. Trabelsi, H., Jamei, M., Zenzri, H., Olivella, S. Crack patterns in clayey soils: Experiments and modeling, International Journal for Numerical and Analytical Methods in Geomechanics. 2012. Vol. 36. No. 11. Pp. 1410–1433.
16. Agus, S.S., Schanz, T. Swelling pressure and total suction of compacted bentonite sand mixtures. In: Bilsel, H., Nalbantoglu, Z. (Eds.), Proceedings of the International Conference on Problematic Soils. 2005. Vol. V1. North Cyprus. Pp. 61–70.
17. van-Genuchten, M.T. A closed form equation for predicting the hydraulic conductivity of unsaturated soils. Soil Science Society of America Journal. 1980. 44. Pp. 892–898.
18. Morel, J.C., Ghavami, K., Mesbah, A. Theoretical and experimental analysis of composite soil blocks reinforced with Sisal fibres subjected to shear. Masonry International. 2000. 13(2). Pp. 54–62.
19. Prabakara, J., Sridharb, R.S. Effect of random inclusion of sisal fibre on strength behaviour of soil. Construction and Building Materials. 2002. Vol. 16. No. 2. Pp. 123–131.
20. Zhang, C.-C., Zhu, H.-H., Shi, B., Wu, F.-D., Yin, J.-H. Experimental Investigation of Pullout Behavior of Fiber-Reinforced Polymer Reinforcements in Sand. Journal of Composites for Construction. 2015. 19. Pp. 11.
21. Bessadok, A., Roudesli, S., Marais, S., Follain, N., Lebrun, L. Alfa fibres for unsaturated polyester composites reinforcement: effects of chemical treatments on mechanical and permeation properties. Composites. 2009. Part A. Vol. 40. No. 2. Pp. 184–195.
22. Lakshmikantha, M.R., Prat, P.C., Ledesma, A. Image analysis for the quantification of a developing crack network on a drying soil. Geotechnical Testing Journal. 2009. 32(6). Pp. 505–515.
23. Lakshmikantha, M.R., Prat, P.C., Ledesma, A. Experimental evidence of size effect in soil cracking. Can. Geotech. 2012. J. Vol. 49. Pp. 264–284.
24. Sanchez, M., Atique, A., Kim, S., Romero, E., Zielinski, M. Exploring desiccation cracks in soils using a 2D profile laser device. Acta Geotechnica. 2013. 8. Pp. 583–596. DOI 10.1007/s11440-013-0272-.
25. Vogel HJ, Hofmann H, Roth K., Studies of crack dynamics in clay soil: I. Experimental methods, results, and morphological quantification. Geoderma. 2005. 125. Pp. 203–211.
26. Vogel, H.J., Hofmann, H., Leopold, A., Roth, K. Studies of crack dynamics in clay soil: II. A physically based model for crack formation. Geoderma. 2005. 125. Pp. 213–223.
27. Tang, C.-S., Shi, B., Liu, C., Suo, W.-B., Gao, L. Experimental characterization of shrinkage and desiccation cracking in thin clay layer, Applied Clay Science, 2011. Vol. 52. No. 1-2. 26. Pp. 69–77.
28. Tang, C.S., Pei, X.J., Wang, D.Y., Shi, B., Li, J. Tensile strength of compacted clayey soil. J. Geotech. Geoenviron. 2014. 141(4). 04014122.
29. Mazars, J., Bažant, Z.P. Cracking and damage: localization and size effect. 1989, Elsevier, New York.
30. Lima, L.A., Grismer, M.E. Application of fracture mechanics to cracking of saline soils. Soil Science. 1994. 158(2). Pp. 86–96. DOI: 10.1097/00010694-199408000-00002
31. Tang, C.-S., Shi, B., Cui, Y.-J., Liu, C., Gu, K. Desiccation cracking behavior of polypropylene fiber-reinforced clayey soil. Canadian Geotechnical Journal. 2012. Vol. 49. No. 9. 31. Pp. 1088–1101.
32. Wei, X., Hattab, M., Bompard, P., Fleureau, J.-M. Highlighting some mechanisms of crack formation and propagation in clays on drying path. Géotechnique. 2016. Vol. 66. No. 4. Pp. 287–300.
33. Zhang, Y., Ye, W.M., Chen, Y.G., Ye, B. Desiccation of Nacl-contaminated soil of earthen heritages in the site of Yar city, Northwest China. Applied Clay Science. 2017. Vol. 124-125. Pp. 1–10.

34. Péron, H., Hueckel, T., Laloui, L., Hu, L.B. Fundamentals of desiccation cracking of fine-grained soils: Experimental characterisation and mechanisms identification. Canadian Geotechnical Journal. 2009. Vol. 46. No. 10. Pp. 1177–1201.
35. Cordero, J.A., Useche, G., Prat, P.C., Ledesma, A., Santamarina, J.C. Soil desiccation cracks as a suction contraction process. Géotechnique Letters. 2017. Vol. 7. No. 4. Pp. 272–278.
36. Wang, L.-L., Tang, C.-S., Shi, B., Cui, Y.-J., Zhang, G.-Q., Hilary, I. Nucleation and propagation mechanisms of soil desiccation cracks. Engineering Geology. 2018. Vol. 238. Pp. 27–35.

Contacts:

Mehrez Jamei, mehjamei@yahoo.fr
Yahya Elassaf, ysalassaf@gmail.com
Anwar Ahmed, bokshe12@yahoo.com
Abdelkader Mabrouk, abdmabs@yahoo.fr